Effect of LCP and rPET as Reinforcing Materials on Rheology, Morphology, and Thermal Properties of *in situ* Microfibrillar-Reinforced Elastomer Composites

Sunan Saikrasun,[1] Panpirada Limpisawasdi,[1] Taweechai Amornsakchai[2]

[1]*Department of Chemistry and Center of Excellence for Innovation in Chemistry, Mahasarakham University, Mahasarakham 44150, Thailand*
[2]*Center for Alternative Energy, Department of Chemistry and Center of Excellence for Innovation in Chemistry, Mahidol University, Bangkok 10400, Thailand*

Received 6 February 2008; accepted 11 November 2008
DOI 10.1002/app.29715
Published online 11 February 2009 in Wiley InterScience (www.interscience.wiley.com).

ABSTRACT: Microfibrillar-reinforced elastomer composites based on two dispersed phases, liquid crystalline polymer (LCP) and recycled poly(ethylene terephthalate)(rPET), and styrene-(ethylene butylene)-styrene (SEBS) were prepared using extrusion process. The rheological behavior, morphology, and thermal stability of SEBS/LCP and SEBS/rPET blends containing various dispersed phase contents were investigated. All blends and LCP exhibited shear thinning behavior, whereas Newtonian fluid behavior was observed for rPET. The incorporation of both LCP and rPET into SEBS significantly improved the processability by bringing down the melt viscosity of the blend system. The fibrillation of LCP dispersed phase was clearly observed in as-extruded strand with addition of LCP up to 20–30 wt %. Although the viscosity ratio of SEBS/rPET system is very low (0.03), rPET domains mostly appeared as droplets in as-extruded strand. The results obtained from thermogravimetric analysis suggested that an addition of LCP and rPET into the elastomer matrix improved the thermal resistance significantly in air but not in nitrogen. The simultaneous DSC profiles revealed that the thermal degradation of all polymers examined were endothermic and exothermic in nitrogen and in air, respectively. © 2009 Wiley Periodicals, Inc. J Appl Polym Sci 112: 1897–1908, 2009

Key words: elastomer; composites; liquid crystalline polymer (LCP); thermal degradation; recycled PET (rPET); thermal stability

INTRODUCTION

Blending two or more polymers is a versatile way of developing new materials with a desirable combination of properties. Among such blending systems, immiscible blends of thermotropic liquid crystalline polymers (TLCPs) with thermoplastics or thermoplastic elastomers (TPEs) have received much attention over the past 2 decades.[1–3] TLCPs are known to possess superior physical properties, such as high strength, good thermal properties, and low melt viscosity. Under appropriate shear or elongational flow field, dispersed TLCP droplets can be elongated and frozen in the matrix after cooling. This type of blend is called *in situ* composite.[4] Two major advantages gained by the addition of small amount of TLCP into a polymer matrix are improved processability and enhancement of mechanical properties. However, the main problem to be investigated for these types of the blends is to find the optimum processing conditions, composition of the blend component, viscosity ratio (dispersed phase to matrix phase), and fabrication techniques to obtain a fibrillar morphology of the dispersed phase. Despite the numerous advantages of TLCP as a minor blend component, which can improve the melt processability and enhance mechanical properties, TLCPs are often too expensive for general engineering applications. On the other hand, there are considerable supplies of engineering plastics in the form of post consumer scraps, which are a low cost source of raw material for forming polymer blends.[5] An alternative way is to find a substitute for TLCPs in fiber-reinforced composite application as a new type of processing route.

Poly(ethylene terephthalate) (PET) is one of the most important polymers for industrial production because of rapid growth in its uses. It is regarded as an excellent material for many applications and is widely used for making containers (bottles) for liquids. It has excellent tensile and impact strength,

Correspondence to: S. Saikrasun (sunan.s@msu.ac.th).
Contract grant sponsor: Office of Commission on Higher Education and Thailand Research Fund; contract grant number: MRG5080415.

chemical resistance, clarity, processability, color ability, and reasonable thermal stability. Nowadays, soft drink bottles are preferentially made with PET. However, there are increasing pressures from the public for recycling of these PET bottles to reduce the demand on land-fill space. The common forms of plastic recycling include incineration with the recovery of thermal energy, transforming the PET waste back to the feed stock and thermomechanical recycling including the formation of PET blends and alloys.[6] Numerous studies have been carried out to investigate the possibilities of recycling PET (mainly bottles) for the production of injection-moldable, extrudable, and thermoformable PET resins that could be used to make structural parts of vehicles, automatives, textiles, food containers, bottles, etc.[7–9] At present, the developed industrial countries are drawing up legislation and special program to promote bottle recycling. There is a continuing need for the availability of efficient, cost-effective recovery and recycling systems that can convert scrap bottles into useful products. Most of recycled PET (rPET) goes into low-end products such as fiberfill for pillows, outwear, polyester foams, and strapping.[10]

So far one of the most important use of rPET is as a blend component. Especially, the blends of rPET with common thermoplastics such as polypropylene[5,11–13] and polyethylene[14–17] based on the concept of *in situ* microfibrillar-reinforced composites (iMFCs)[18] have received much attention during the last decade. However, to the authors' knowledge, very limited information is available with regard to the rPET-TPE blends and a direct comparison of phase behavior and properties between TPE/LCP and TPE/rPET blend system has not been investigated. In this study, styrene-(ethylene butylene)-styrene (SEBS) triblock copolymer, a TPE, was melt blended with LCP and rPET using extrusion process. Rheological behavior in the molten state, morphology and thermal properties of SEBS/LCP, and SEBS/rPET blend systems were investigated and compared. The main goal of this study is to explore the potential of rPET as low-cost and easily available reinforcing material for microfibrillar-reinforced elastomer composites. The results for the SEBS/rPET system were compared with those of the SEBS/LCP blend system.

EXPERIMENTAL

Materials

The polymer dispersed phases used in this work were Rodrun LC3000, a TLCP, supplied by Unitika Co. (Tokyo, Japan) and rPET collected from post consumer soft drink bottles. Rodrun LC3000 is a copolyester of 60 mol % *p*-hydroxy benzoic acid (HBA) and 40 mol % PET with a melting point of 220°C and a density of 1.41 g/cm^3. The rPET bottles were cleaned and cut into small pieces with dimension of about 3 mm × 3 mm. The melting temperature of rPET is found to be 252–255°C (examined by using DSC). The matrix phase used in this study was SEBS triblock copolymer (Kraton G1650) consisting a styrene/rubber weight percent ratio of 29/71. The SEBS polymer matrix was purchased from Toyota Tsusho (Thailand) Co. The chemical structures of all the polymers used in the present study are shown in Scheme 1. All materials were dried in a vacuum oven at 70°C for at least 12 h before use. In this article, Rodrun LC3000 liquid crystalline polymer was represented by LCP.

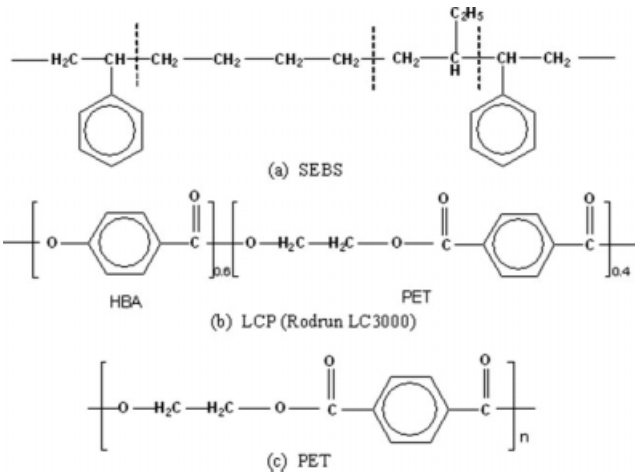

Scheme 1 Chemical structures of (a) SEBS, (b) LCP (Rodrun LC3000), and (c) PET.

Blend preparation

The SEBS/LCP and SEBS/rPET blends at various compositions were prepared with a single screw extruder [Haake Rheomex, Thermo Electron (Karlsruhe) GmbH, Karlsruhe, Germany], with a screw diameter of 16 mm, length-to-diameter (L/D) ratio of 25, a die diameter of 2 mm, and a screw speed of 100 rpm. The temperature profiles for preparation of SEBS/LCP and SEBS/rPET were 190-220-220-225°C and 190-250-255-260°C, respectively. The temperature profiles shown here represent the temperatures at hopper zone, two barrel zones and heating zone in the die head, respectively. The extruded strand was immediately quenched in a water bath and subsequently dried in a vacuum oven. The sample codes of the extruded strand blends are designated as SEBS-*x*LCP or SEBS-*x*rPET where *x* depicts the content of LCP or rPET in wt %.

Rheological measurements

Measurements of rheological properties in the molten state for all the neat components and the blends

were carried out with a plate-and-plate rheometer (Physica Anton Paar, MCR5000, Physica Messtechnik GmbH, Stuttgart, Germany). The extruded strands were cut into pellets and compression-molded at 200°C into a sheet about 1.5 mm thick. The sheet was then punched into a disk 25 mm in diameter. The complex viscosity (η*), storage modulus (G'), and loss modulus (G'') of all specimens were measured in the oscillatory shear mode with the strain amplitude of 5% within the angular frequency (ω) range from 0.6 to 500 rad s^{-1}. The measuring temperatures for the SEBS/LCP and SEBS/rPET systems were 225 and 260°C, respectively. The gap between the two plates was set at 0.9 mm.

Morphological characterization

The fracture surfaces of both types of extruded strand blends were observed under the scanning electron microscope (SEM) (Jeol; JSM-6460LV, Tokyo, Japan) operated with an accelerating voltage of 15 kV. Before examination, the extruded strands were immersed in liquid nitrogen for 30 min and fractured. The specimens were sputter-coated with gold for enhanced surface conductivity.

Measurement of thermal decomposition behavior

The thermogravimetric analysis (TGA) was carried out using TA instruments, SDT Q600 (Luken's drive, New Castle, DE). The pellets, 8–10 mg, cut from the extruded strands were loaded in alumina crucible. The samples were non-isothermally heated from ambient temperature to 1000°C at a heating rate of 10°C/min. The TGA was performed in nitrogen and in air with the flow rate of 100 mL/min. The TG and DSC data were simultaneously recorded online in TA instrument's Q series explorer software. The analyses of the TG data were done using TA Instrument's Universal Analysis 2000 software (version 3.3B).

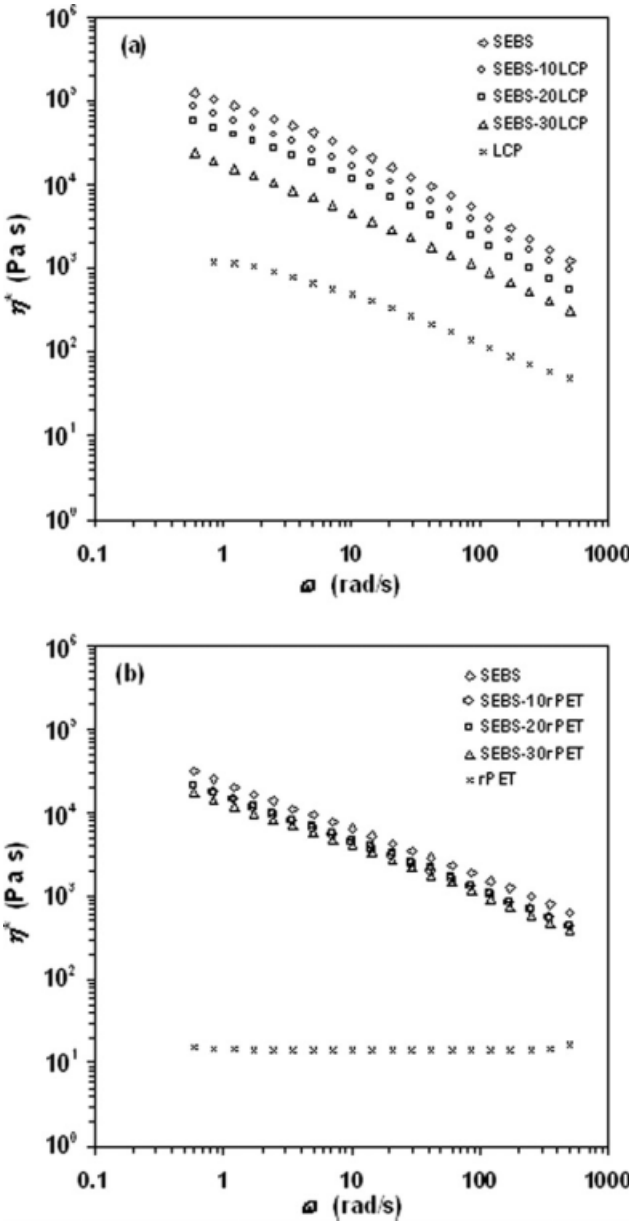

Figure 1 η* versus ω for (a) SEBS/LCP and (b) SEBS/rPET blends containing various dispersed phase contents, measured at 225°C and 260°C, respectively.

RESULTS AND DISCUSSION

Rheological behavior in the molten state

In this study, different temperature profiles were used for preparation of the two types of blends because of different melting temperature of the dispersed phases. Rheological measurements in the molten state of SEBS/LCP and SEBS/rPET blends were carried out at 225°C and 260°C, respectively. Figure 1 shows the frequency (ω) dependence of complex viscosity (η*) for all analyzed samples. All neat and blend samples, except rPET, exhibit shear thinning behavior; the viscosity decreases with increasing shear rate (or shear frequency) because of the shear-induced chain orientation, leading to a reduction in the chain entanglement density. We will now consider the SEBS-LCP system first [Fig. 1(a)]. SEBS displays the highest viscosity whereas LCP displays the lowest viscosity. SEBS-LCP blends show viscosity in between these ranges and the viscosity decreases with increasing LCP content. This indicates that the addition of a small amount of LCP into SEBS matrix improves melt processability significantly. For SEBS-rPET system, similar trend is seen. However, despite rPET has much lower viscosity than LCP, addition of rPET into SEBS does not decrease the viscosity to the same extent that LCP does.

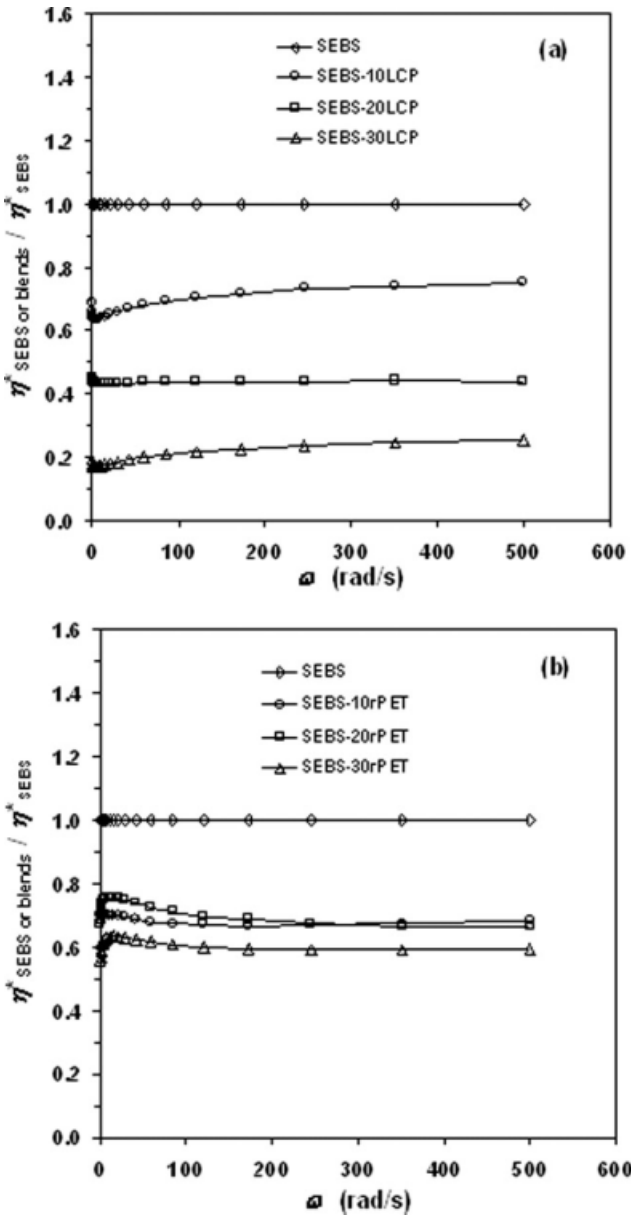

Figure 2 Relative η* versus ω for (a) SEBS/LCP and (b) SEBS/rPET blends containing various dispersed phase contents, measured at 225°C and 260°C, respectively.

The relative viscosity, defined as the ratio of the viscosity of SEBS or the blends to that of the matrix phase, was calculated and presented in Figure 2, to evaluate the potential of rPET as the processing lubricant component compared with that of LCP. For the SEBS/LCP system, the decrease in the relative viscosity strongly depends on LCP contents as seen from Figure 2(a). The reduction of the relative viscosity for the SEBS/LCP system enhances with LCP loading, indicating that higher the LCP content the higher the improvement in the melt processability. Similarly for SEBS/rPET system [Fig. 2(b)], the relative viscosity of the rPET-containing blends is also lower than that of the neat SEBS. It is interesting to note that the reduction of relative viscosity for both types of the blends with 10 wt % dispersed phase is comparable (the relative viscosity reduces by 20–25% than that of the neat SEBS). With further addition of rPET up to 20–30 wt %, the efficiency of rPET as the processing aid for the blend system is not as good as that containing the same amount of LCP. However, the incorporation of small amount of rPET into SEBS significantly reduces the melt viscosity of the blend system.

Because both SEBS-LCP and SEBS-rPET are immiscible, the reduction in viscosity of the blend systems would be similar to the action of external lubricant. LCP is known to have good melt lubricity and addition of LCP could reduce the viscosity of the system by reducing friction at the interface of the polymer and the surface of the equipment or between the interface of polymer streams. The fact that the low viscosity of rPET does not translate to the low viscosity of the blend would suggest that the lubrication capability of rPET itself is not as good as LCP. However, at about 10% content, rPET could reduce the viscosity of SEBS in the same extent as LCP.

The elastic and viscous characteristics of the blend system can be considered from the plots of the storage modulus (G') and the loss modulus (G''), respectively, as a function of ω (Figure 3). The values of G' and G'' at low frequency generally provide information about long-range (beyond entanglement distance) relaxation, whereas the values at high frequency provide information about short range (motion with entanglement) relaxation.[19] As seen from Figures 3(Ia) and (Ib), G' increases with increasing ω indicating a dependence of G' on the time scale of molecular motion. For both the blend systems, the neat SEBS matrix shows the highest value of G' whereas G' of LCP and rPET display the lowest values among the corresponding blend samples. The decrease in G' is observed for the SEBS/LCP and SEBS/rPET blend systems with increase in the concentration of the LCP or rPET as a result of the contribution of the dispersed phases. This means that LCP and rPET in the polymer matrix play a role in promoting the chain mobility leading to a decrease in chain rigidity. However, although the G' of rPET is much lower than that of SEBS, a slight reduction of G' is observed for the blends containing 10–30 wt % rPET. For the LCP-containing blend system, the reduction in G' is clearly observed, indicating that the change in elastic properties of SEBS matrix by blending with LCP is more pronounced than that by blending with rPET. This should arise from the fact that the LCP molecules contain rigid parts, which could slide pass each other easily and results in good lubricity. On the other hand, the chains of rPET are more flexible and would take

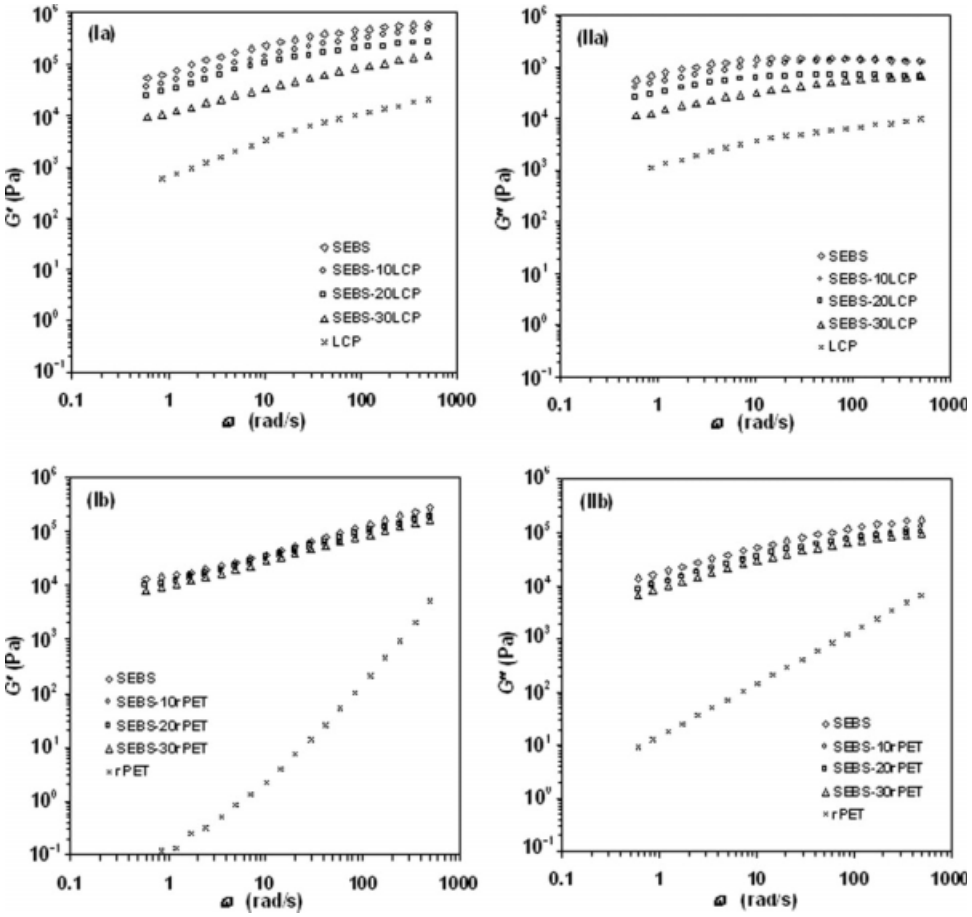

Figure 3 G' (column I) and G'' (column II) versus ω for (a) SEBS/LCP and (b) SEBS/rPET blends containing various contents of dispersed phase. The measurements of G' and G'' for SEBS/LCP and SEBS/rPET blends were carried out at 225°C and 260°C, respectively.

random coil configuration. Chain entanglements are likely to occur and this will be less effective in lubricating the system. Interestingly, the elastic characteristics of rPET [Fig. 3(Ib)] are strongly affected by the applied frequency as seen from the dramatical increase in G' with increasing frequency because the elastic energy stored in the molecules is greater when the deformation from a random coil configuration takes place within shorter times.[20] As a consequence, the G' of rPET is close to those of SEBS and the blends at high frequency.

The viscous characteristics (G'') for both blend systems is found to decrease with increasing dispersed phase contents as seen from Figures 3(IIa) and (IIb) for SEBS/LCP and SEBS/rPET blends, respectively. At the same composition for both types of the blends, G' values of the neat SEBS, LCP, and all blends are higher than the corresponding G'' values in the whole frequency range. This indicates that the elastic characteristics for these samples are dominant factor. In turn, it clearly appears that for rPET analyzed, the G''dominates with respect to the G', especially in the low frequency range. This arises from the fact that, by comparing with LCP, the molecular weight of rPET is relatively low and it has narrow molecular weight distribution, enabling the chain motion with low level of molecular entanglement. Unfortunately, the molecular weights of both the dispersed phases could not be numerically compared because so far the molecular weight of LCP is not obtainable, because no solvent is found to dissolve this polymer. The dominant viscous characteristic of rPET observed in this study is in well accordance with those of the vergin PET and bottle grade PET reported by Daver et al.[20] and Incarnato et al.[21]

It is generally known that the morphology of immiscible blend is governed by the viscosity ratio of the dispersed phase to the matrix phase. For simple shear flow, fibrillar morphology is predicted to occur if the viscosity ratio is lower than unity.[22–24] In general, the lower the viscosity ratio, the higher the possibility of forming fibrillar morphology would be. The viscosity ratio will now be examined as it is one of the criteria, which have been used to determine the possibility of fibril formation. The viscosity ratios

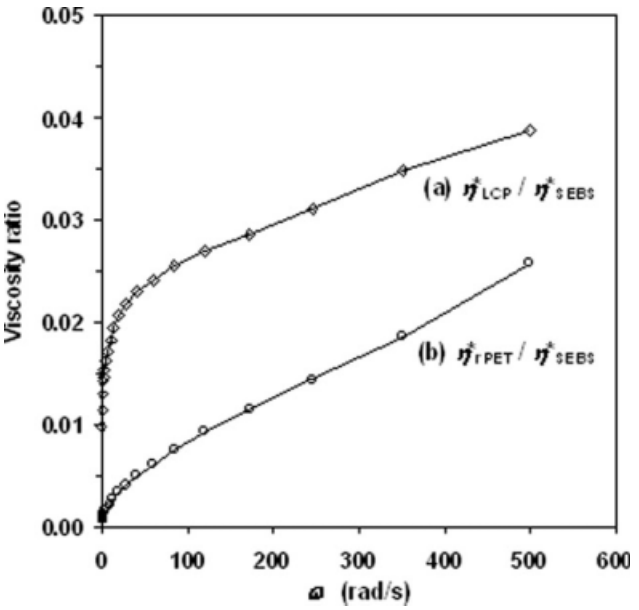

Figure 4 Viscosity ratios versus ω for (a) SEBS/LCP and (b) SEBS/rPET blending systems, measured at 225°C and 260°C, respectively.

as a function of frequency for the SEBS/LCP at 225°C and SEBS/rPET blend systems at 260°C were evaluated and presented in Figure 4. It is seen that the viscosity ratios of both the blend systems are lower than 0.05 over the entire frequency region investigated. The viscosity ratio of the SEBS/LCP system increases sharply first from 0.01 to 0.02 within the frequency range of 0–30 rad s and then increases gradually as the frequency increases further. The increase of viscosity ratio with increasing frequency arises from the faster drop of the viscosity of SEBS than that of LCP in the high frequency range. Similarly, the viscosity ratio for the SEBS/rPET system progressively increases with increasing frequency. However, the viscosity ratio of the SEBS/rPET system is much lower than that of the SEBS/LCP system at all measuring frequencies. The difference in viscosity ratio arising from the different dispersed phase viscosity is expected to affect the fibrillation of the LCP and the rPET. On the basis of the obtained results of viscosity ratios, it may be expected that both LCP and rPET can form the fibrillation morphology and the better fibrillation should be observed in the rPET-containing blends.

Morphology

It is well known that the final properties of the iMFCs depend on its phase morphology, which is affected by several important factors such as rheological behavior, composition, interfacial tension, processing condition, and fabrication techniques. In the present study, the morphology of the fracture surface was studied by means of SEM. Figure 5 shows the SEM micrographs of the fracture surfaces for the SEBS/LCP and SEBS/rPET extruded strands containing various LCP and rPET contents. In the LCP-containing blend with 10 wt % LCP [Fig. 5(Ia)], most of the LCP domains appeared as droplets, and few elongated LCP domains are observed. The fibrillation of LCP domains is clearly observed in the blend with 20 wt % LCP [Fig. 5(Ib)]. However, with the addition of LCP up to 30 wt %, some lamellar structure is observed because of the coalescence of the liquid LCP threads that occur during extrusion. The lamellar structure is also observed in other LCP-containing blend systems with incorporation of high LCP concentration.[25–27]

In the case of the SEBS/rPET system, most of the rPET domains in SEBS-10rPET appear as small droplets with diameter of about 0.5–1 μm and the diameter of the rPET domains slightly increases with rPET loading. Some elongated rPET domains are also observed in the SEBS/rPET blends. In addition, limited coalescence of rPET domains are observed in the SEBS-30rPET extruded strands. Interestingly, the domain size of the rPET is much smaller than that of the LCP. According to the results of viscosity ratio shown earlier, Figure 4, it may be expected, from the low viscosity ratios for the SEBS/LCP and the SEBS/rPET systems, that these blend systems will have fibrillar morphology. However, the morphological results from the present study clearly show that good fibrillar morphology is obtained only with the SEBS/LCP system. The fact that rPET break down into small droplets may be due to the high viscosity of the system (Fig. 1) and limited coalescence. Furthermore, the difference in morphology of the SEBS/LCP and the SEBS/rPET systems could be explained as follows. Generally, deformation of the dispersed-phase droplets into fibrillation structures or coalescence of the dispersed-phase domains depends on the ratio between the viscous forces (that tend to elongate the droplets) and the interfacial forces (that tend to keep the drop spherical). This ratio is frequently described by the Capillary number (C_a), which is defined by[28]

$$C_a = \frac{\eta_m \gamma}{(\sigma/b)} \quad (1)$$

where η_m is the viscosity of the matrix, $\dot{\gamma}$ the shear rate, b the initial diameter of dispersed droplets, and σ the interfacial tension between the matrix and dispersed phase. In the simple shear flow of Newtonian fluids, a dispersed droplet will be elongated if $C_a > 0.5$, indicating that the ratio of shear stress and the interfacial energy should be larger than half.[28] The influence of the capillary number on the stability of the dispersed phases especially for LCP

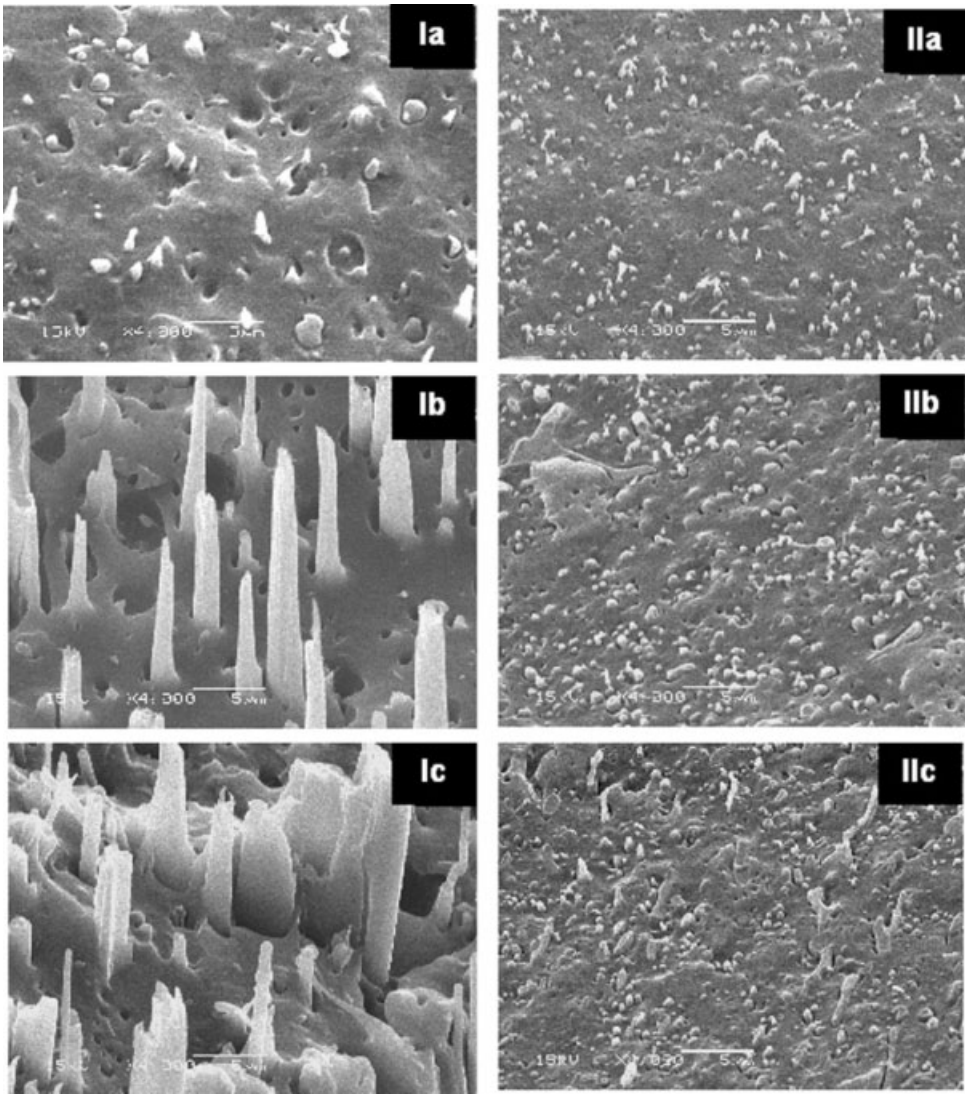

Figure 5 SEM micrographs of the fracture surface for SEBS/LCP (column I) and SEBS/rPET (column II) blends containing (a) 10, (b) 20, and (c) 30 wt % dispersed phase.

morphology has been studied by a number of researchers.[29,30] The results of their study indicate the influence of both viscous and interfacial forces on the final morphology, confirming the importance of Capillary number. In the case of SEBS/rPET system, even if the viscosity ratio is lower than 0.03, the fibrillation of the rPET domains is not clearly observed in as-extruded strand. According to eq. (1), there can be two possibilities that cause the Capillary number to be low. They are small initial diameter of the dispersed phase and the high interfacial tension. The former is apparent from Figure 5. rPET droplets are so small and coalesence of droplets does not occur even at high rPET content. The fibrilation of rPET therefore does not occur. However, thermotropic LCPs are essentially rigid-rod long chain molecules with some irregularity or flexibility incorporated into the polymer chain to lower the melting point below the decomposition temperature. The rigid-rod molecular structure allows these materials to exhibit molecular order in a liquid mesophase resulting in a tendency toward easy orientation in the flow direction. In contrast, the random coil structure and relatively flexible structure of rPET tend to appear in the molten state. Thus, the fibrillation tendency of rPET is not as good as that of highly-orientated nature LCP.

Thermal decomposition behavior

Normally, polymers must encounter elevated temperatures at almost every stage in manufacturing, compounding, and processing stages, in service, and during repairing step. Therefore, an understanding of thermal stability and thermal decomposition behavior of polymer is an essential information for development and extension of their applications. In the present study, TGA was performed to gain some

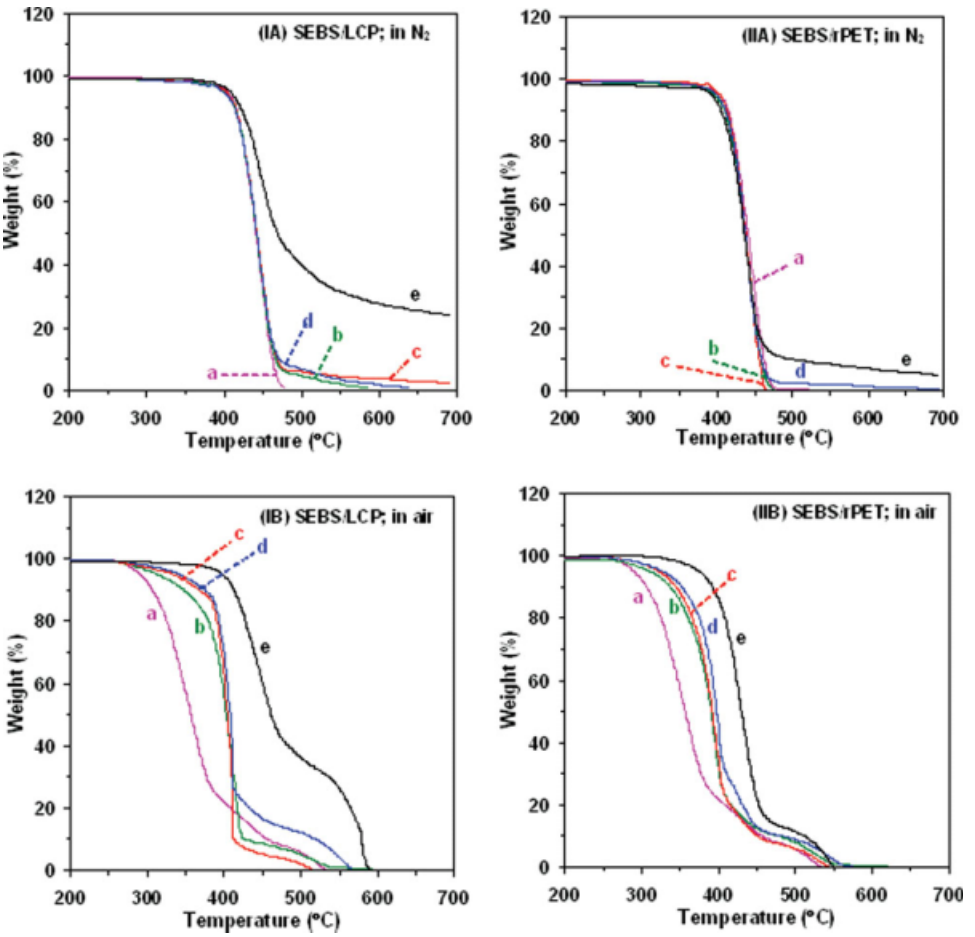

Figure 6 Dynamic TG curves of SEBS/LCP (column I) and SEBS/rPET (column II) blends containing (a) 0, (b) 10, (c) 20, (d) 30, and (e) 100 wt % LCP or rPET at a heating rate of 10°C/min in nitrogen (row A) and in air (row B). [Color figure can be viewed in the online issue, which is available at www.interscience.wiley.com.]

understanding of the effect of the LCP and the rPET on thermal decomposition of the SEBS/LCP and the SEBS/rPET blends. The non-isothermal TG curves of the two blending systems are presented in Figure 6. The TG measurements were carried out in nitrogen and in air at a heating rate of 10°C/min.

TG results of the SEBS/LCP blends [Fig. 6(IA)] obtained in nitrogen will be considered first. The non-isothermal TG profile of SEBS reveals only a single weight-loss step at the temperature range around 400–480°C. The single weight-loss step of SEBS in nitrogen revealed in this study, which corresponds mainly to the chain scission at the boundary of the polystyrene-olefin phase, is similar to that of SEBS under non-isothermal heating in argon flow reported by Zucolotto et al.[31] Although the blend system may be complicated due to the presence of many copolymer components, a single degradation step similar to the neat SEBS matrix is observed for the blends containing 10–30 wt % LCP. The onset of decomposition in nitrogen seems not to be affected by the LCP loading. In the LCP-containing blends, the degradation mechanism additionally involves the removal of ester, ethylene groups, and hydrogen atoms in the polymer chains of LCP.[32] That is, there are more than one reaction for the decompositon. In the case of LCP, the first thermal degradation mainly occurs at the PET block, whereas the second degradation process could be attributed to the degradation of the HBA block.[32,33] It is seen that no char residues were left for the neat SEBS whereas the amount of char residues increases with increasing the LCP contents. The increase in char residues arises from the increase in the HBA block (by increasing amount of LCP content), which will decrease the number of hydrogen atoms and retard the formation of volatile degraded products.[34] Moreover, the formation of char residues is probably due to the branch formation and crosslinking of the product obtained mostly from the HBA unit during the thermal degradation under nitrogen.

Under dynamic heating in air [Fig. 6(IB)], the thermal degradation of the SEBS, the LCP and their blends occur in two steps. The neat SEBS exhibits the first weight-loss step at 250–380°C, whereas the first major weight-loss of the LCP occurs around

400–500°C. For the thermal degradation of SEBS in air, the chain degradation, scission and oxidation occur primarily at the boundary of styrene-olefin phases, giving rise to the formation of acetone end groups on the styrene units and carboxylic acids on the olefin chain ends.[35] Concurrent and further reaction give rise to the formation of anhydrides and perester/acids in the longer term together with vinyl and α, β-unsaturated carbonyl products, predominantly carboxylic acids. The olefin phase was found to exhibit severe oxidation and crosslinking associated with the initial formation of unstable primary hydroperoxide species. The presence of hindered phenolic antioxidant and phosphate were also higher synergistic in inhibiting oxidation and separation at the boundaries by destroying the acetophenone end groups and preventing excimer disaggreation. Note that, in air, no char residues of the neat polymers and the blends were left within the experimental temperature.

In the case of SEBS/rPET blend system in nitrogen [Fig. 6(IIA)], the single-step weight-losses are observed for the neat polymers and the blends at 380–460°C. Several studies have been conducted on the thermal degradation products of PET,[36–39] which indicate that the thermal degradtion of PET is initiated by chain scission of ester-linkage, yielding carboxyl and vinyl ester groups. In air [Fig. 6(IIB)], at least two weight-loss steps are observed for all samples indicating that the degradation process is more complex in air than in nitrogen.

To compare the dispersed phase-content dependence of thermal stability for the two types of blends in more quantitative way, the thermal decompositon data in nitrogen and in air are compared and summarized in Table I. T_{onset} represents the onset degradation temperature. T_{max} represents the temperature at the maximum weight-loss rate, $(d\alpha/dt)_{max}$. The subscripts 1 and 2 represent the first stage and the second stage of thermal degradation, respectively. In nitrogen, no significant difference in T_{onset} between the SEBS/LCP and SEBS/rPET blends are observed when compared at the same blend composition. T_{max1} of the LCP-containing blends are slightly higher than that of the corresponding rPET-containing blends. It is noticed that at the same composition, $(d\alpha/dt)_{max}$ of the SEBS/LCP blend systems are lower than those of the SEBS/rPET blend systems. This indicates that incorporation of the LCP into SEBS results in somewhat higher thermal resistance when compared with the rPET-containing blends at the same composition.

In air, it is interesting to note that T_{onset} and T_{max1} of the two types of blends are much higher than those of the matrix but are lower than those of the corresponding dispersed phase. This means that incorporation of the LCP and rPET into the SEBS matrix effectively enhance the thermal stability in air

TABLE I
Nonisothermal Decomposition Characteristics of SEBS/LCP and SEBS/rPET Blends in Nitrogen and in Air

LCP or rPET content (wt %)	SEBS/LCP blending system					SEBS/rPET blending system				
	T_{onset} (°C)	T_{max1} (°C)	T_{max2} (°C)	$(d\alpha/dt)_{max1}$ (%/min)	$(d\alpha/dt)_{max2}$ (%/min)	Char yield at 600°C (wt %)	T_{onset} (°C)	T_{max1} (°C)	T_{max2} (°C)	$(d\alpha/dt)_{max1}$ (%/min)	$(d\alpha/dt)_{max2}$ (%/min)	Char yield at 600°C (wt%)
In nitrogen												
0	417	448	–	20.4	–	0.00	417	448	–	20.4	–	0.00
10	417	445	–	20.0	–	0.38	416	440	–	25.6	–	0.00
20	418	451	–	23.2	–	0.05	419	439	–	30.1	–	0.00
30	417	437	–	20.5	–	0.15	419	443	–	24.0	–	0.14
100	419	448	–	10.5	–	27.6	414	441	–	20.8	–	7.13
In air												
0	310	354	528	11.0	1.99	0.00	310	354	528	11.0	1.99	0.00
10	385	410	518	33.4	1.18	0.02	366	391	523	19.7	1.65	0.03
20	402	405	527	52.8	1.63	0.00	367	387	538	19.9	1.62	0.00
30	401	408	552	48.8	2.57	0.00	377	400	549	33.3	1.79	0.00
100	410	449	573	9.58	19.8	0.00	399	433	553	16.3	5.16	0.00

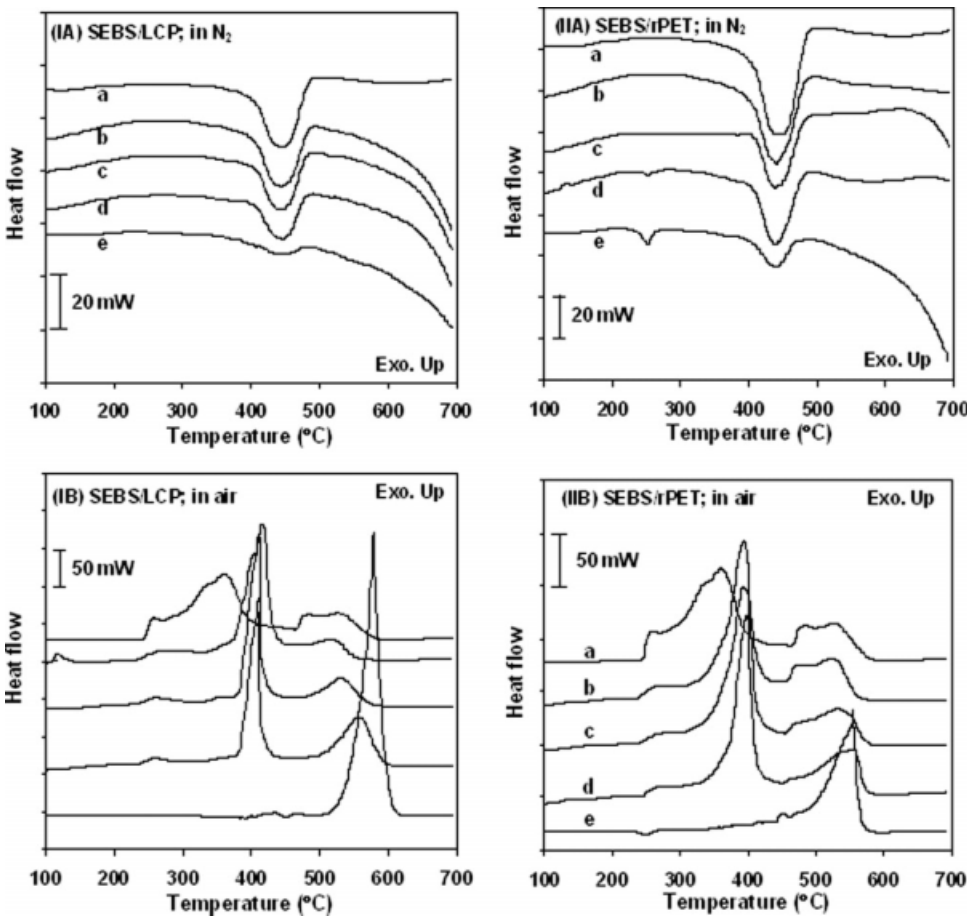

Figure 7 Simultaneous DSC curves of SEBS/LCP (column I) and SEBS/rPET (column II) blends containing (a) 0, (b) 10, (c) 20, (d) 30, and (e) 100 wt % LCP or rPET at a heating rate of 10°C/min in nitrogen (row A) and in air (row B).

but not in nitrogen. It is found that T_{onset} and T_{max1} of the blends with 10–30 wt % LCP are shifted by about 75–90°C and 50–55°C, respectively, higher than those of the neat matrix, whereas the respective T_{onset} and T_{max1} of the blends with 10–30 wt % rPET are shifted about 56–67°C and 34–46°C higher than those of the neat SEBS. It is seen that $(d\alpha/dt)_{max1}$ of the LCP- and rPET-containing blends are higher than that of the neat matrix and they decrease with increasing dispersed phase content, indicating the rapid weight-loss process with more complex degradation mechanism. Normally, the thermal stability of polymer in air is somewhat lower than that in nirogen. However, the situation that polymer has been exposed in air is more common than in nitrogen during real processing and application. Note that $(d\alpha/dt)_{max2}$ of the LCP and rPET dispersed phases are much higher than that of the matrix phase whereas T_{max2} seem to mostly increase with the addition of LCP and rPET dispersed phases.

Simultaneous DSC data of thermal decomposition

The DSC traces of degradation for the SEBS, LCP, rPET, and the blends in nitrogen and in air are shown in Figures 7. The DSC curve of SEBS in nitrogen [Fig. 7(IA)] shows a minimum degradation endotherms at (450°C whereas that of the LCP exhibits a broad degradation endotherm with a peak minimum at 430°C. It is noticed that the peak minimum of the SEBS is little affected by the incorporation of LCP. In the case of SEBS/rPET [Fig. 7(IIA)], the exothermic peak, known as "cold crystallization," is not clearly observed, whereas the endothermic peak associated with the fusion of the crystalline fraction is observed at about 275°C. In addition, the largest endothermic peak of rPET is observed at about 460°C corresponding to the degradation process of rPET. However, although the degradation temperature of rPET is higher than that of the neat SEBS, the incorporation of rPET into SEBS does not seem to influence the degradation temperature of the blend in nitrogen.

Under heating in air, the exothermic degradation process is observed for all the samples due to the fact that the concurrent and further degradation mechanisms in air tend to involve the formation reaction. SEBS shows a very broad degradation endotherm that stretches from 250 to 560°C. It is

TABLE II
Simultaneous DSC Data of SEBS/LCP and SEBS/rPET Blends Under Thermal Degradation in Nitrogen and in Air

LCP or rPET content (wt %)	SEBS/LCP blending system				SEBS/rPET blending system			
	T_m (°C)	ΔH_m (kJ/g)	T_d (°C)[a]	ΔH_d (kJ/g)	T_m (°C)	ΔH_m (kJ/g)	T_d (°C)[a]	ΔH_d (kJ/g)
In nitrogen								
0	–	–	449	1.08	–	–	449	1.08
10	–	–	445	0.83	–	–	441	0.85
20	–	–	444	0.73	–	–	439	0.63
30	–	–	446	0.71	253	6.15	439	0.56
100	–	–	436	0.12	251	0.04	437	0.20
In air								
0	–	–	360	0.80	–	–	360	0.80
10	–	–	416	6.75	–	–	394	4.05
20	–	–	411	5.68	–	–	393	4.28
30	–	–	411	2.54	–	–	397	3.32
100	–	–	579	6.79	251	0.04	555	3.18

[a] Under heating in air, T_d reported here associates with the first major exothermic peak.

interesting to note that an extremely sharp exotherm is noticed at 400°C with addition of the LCP. At high concentration of LCP (20–30 wt % LCP), the second minor exotherm corresponding to the degradation process of LCP is observed. Interestingly, although LCP starts to degrade in the first step at the temperature range of 400–500°C, the exotherm associated with this region is not observed. The simultaneous data of both blend systems are also quantitatively presented in Table II. T_m and ΔH_m represent the melting temperature and heat flow of melting process, respectively, whereas T_d and ΔH_d represent the peak temperature and heat flow, respectively, associated with the thermal degradation process. In nitrogen, incorporation of the LCP or rPET into SEBS seems to affect little the T_d of the blends. In air, T_d of the blends are much higher than those of the polymer matrix. It is seen that ΔH_d of the blends decreased mostly with LCP or rPET loading because of the dilution effect of the polymer matrix. Moreover, at the same concentration of the dispersed phase, the extent of heat flow is much higher in air than in nitrogen. This indicates that there are not only typically thermal degradation reaction but also thermooxidative reaction, which additionally occurs in air.

CONCLUSIONS

In this work, SEBS *in situ* reinforced with two types of reinforcing materials, LCP and rPET, were prepared. The influence of LCP and rPET dispersed phases on rheology, morphology and thermal stability of the elastomer composites was investigated. It was found that the incorporation of small amount of LCP and rPET (10 wt %) into SEBS significantly reduces the melt viscosity of the blend system. At higher concentration, only LCP that continues to lower the viscosity of the blend system further whereas much less effect was observed for rPET. The large reduction in viscosity in LCP containing system is due to its inherent lubricating property. SEBS/LCP displays fibrillar morphology at 20 and 30 wt % LCP whereas SEBS/rPET does not. The incorporation of LCP or rPET into the elastomer matrix was found to retard the thermal degradation significantly in air but not in nitrogen. These demonstrate the high potential of using rPET in replacing the more expensive LCP as processing aids and also to improve thermal resistance of SEBS.

The authors acknowledge the financial support from the Center of Excellence for Innovation in Chemistry (PERCH-CIC), Commission on Higher Education. Ministry of Education is also gratefully acknowledged. Finally, the authors thank Professor Sauvarop Bualek-Limcharoen for the gift of Rodrun LC3000 liquid crystalline polymer.

References

1. Tjong, S. Mater Sci Eng 2003, R41, 1.
2. Arcierno, D.; Collyer, A. A., Eds. Rheology and Processing of Liquid Crystalline Polymers; Chapman and Hall: London, 1996.
3. Dutta, D.; Fruitwala, H.; Kohli, A.; Weiss, R. A. Polym Eng Sci 1990, 30, 1005.
4. Kiss, G. Polym Eng Sci 1987, 27, 410.
5. Friedrich, K.; Evstatiev, M.; Fakirov, S.; Evstatiev, O.; Ishii, M.; Harrass, M. Compos Sci Technol 2005, 65, 107.
6. Fung, K. L.; Li, R. K. Y. Polym Test 2005, 24, 863.
7. Gurudatt, K.; De, P.; Rakshit, A. K.; Bardhan, M. K. J Indust Textiles 2005, 34, 167.
8. Eric, K. Mater World 1997, 5, 525.
9. Seris, R. Recycling of PET, Polymer Recycling: Science Technology and Application; John Wiley & Sons: Chichester, 1998, 119.

10. Arroyo, M. In Thermoplastic Polyesters: Handbook of Thermoplastics; Olabisi, O.; Ed.; Marcel Decker Inc.: New York, 1997.
11. Taepaiboon, P.; Junkasem, J.; Dungtungee, R.; Amornsakchai, T.; Supaphol, P. J Appl Polym Sci 2006, 120, 1173.
12. Fuchs, C.; Bhattacharyya, D.; Fakirov, S. Compos Sci Technol 2006, 66, 3161.
13. Santos, P.; Pezzin, S. H. J. Mater Process Technol 2003, 517, 143.
14. Evstatiev, M.; Fakirov, S.; Krasteva, B.; Friedrich, K.; Covas, J. A.; Cunha, A. M. Polym Eng Sci 2002, 42, 826.
15. Pawlak, A.; Morawiec, J.; Pazzagli, F.; Pracella, M.; Galeski, A. J Appl Polym Sci 2002, 86, 1473.
16. Ávila, A. F.; Duarte, M. V. Polym Degrad Stab 2003, 80, 373.
17. Zhang, H.; Guo, W.; Yu, Y.; Li, B.; Wu, C. Eur Polym J 2007, 43, 3662.
18. Evstatiev, M.; Fakirov, S. Polymer 1992, 33, 877.
19. Hsieh, T. T.; Tiu, C.; Hsieh, K. H.; Simon, G. P. J Appl Polym Sci 2000, 77, 2319.
20. Daver, F.; Gupta, R.; Kosior, E. J Mater Proc Technol 2008, 204, 397.
21. Incarnato, L.; Scarfato, P.; Di Maio, L.; Acierno, D. Polymer 2000, 41, 6825.
22. Isayev, A. I.; Modic, M. Polym Compos 1987, 8, 158.
23. Blizard, K. G.; Baird, D. G. Polym Eng Sci 1987, 27, 653.
24. Mehta, A.; Isayev, A. I. Polym Eng Sci 1991, 31, 963.
25. Verhoogt, H.; Willems, C. R. J.; Van Dam, J.; De Boer, A. P. Polym Eng Sci 1993, 33, 754.
26. Saikrasun, S.; Bualek-Limcharoen, S.; Kohjiya, S.; Urayama, K. J Appl Polym Sci 2003, 89, 2676.
27. Saikrasun, S.; Amornsakchai, T. J Appl Polym Sci 2006, 101, 1610.
28. Seo, Y.; Kim, K. U. Polym Eng Sci 1998, 38, 596.
29. Postema, A. R.; Fenis, P. J. Polymer 1997, 38, 5557.
30. Chan, C. K.; Whitehouse, C.; Gao, P.; Chai, C. K. Polymer 1997, 42, 7847.
31. Zucolotto, V.; Avlyanov, J.; Mattoso, L. H. C. Polym Composite 2004, 25, 617.
32. Saikrasun, S.; Wongkalasin, O. Polym Degrad Stab 2005, 88, 300.
33. Sato, H.; Kikuchi, T.; Koide, N.; Furuya, K. J Appl Pyrolysis 1996, 37, 173.
34. Li, X. G.; Huang, M. R.; Guan, G. H.; Sun, T. Polym Int 1998, 46, 289.
35. Allen, N. S.; Edge, M.; Wilkinson, A.; Liauw, C. M.; Mourelatou, D.; Barrio, J.; Martinez-Zaporta, M. A. Polym Degrad Stab 2001, 71, 113.
36. Girija, B. G.; Sailaja, R. R. N.; Madras, G. Polym Degrad Stab 2005, 90, 147.
37. Villain, P.; Coudane, J.; Vert, M. Polym Degrad Stab 1995, 49, 393.
38. Williams, P. T.; Williams, E. A. Energy Fuels 1999, 13, 188.
39. Dzieciol, M.; Trzeszczynski, J. J Appl Polym Sci 1998, 69, 2377.